Electronic Supporting Information for:

Three coordinate models for the binuclear Cu_A electron-transfer site

Shiyu Zhang and Timothy H. Warren*

Department of Chemistry, Georgetown University, Box 571227, Washington, DC 20057, United States

Contents

General Experimental Details

All experiments were carried out in a dry nitrogen atmosphere using an MBraun glovebox and/or standard Schlenk techniques. 4 Å molecular sieves were activated *in vacuo* at 180 ºC for 24 h. Dry toluene, fluorobenzene and dichloromethane were purchased from Aldrich and were stored over activated 4 Å molecular sieves under nitrogen. Tetrahydrofuran (THF) was first sparged with nitrogen and then dried by passage through activated alumina columns. Pentane was first washed with conc. HNO_3/H_2SO_4 to remove olefins, stored over $CaCl_2$ and passed through activated alumina column. All deuterated solvents were sparged with nitrogen, dried over activated 4 Å molecular sieves and stored under nitrogen. ^1H and ^{13}C NMR spectra were recorded on Varian 400 MHz spectrometer. All NMR spectra were recorded at room temperature unless otherwise noted and were indirectly referenced to TMS using residual solvent signals as internal standards. Elemental analyses were performed on a Perkin-Elmer PE2400 microanalyzer in our laboratories, and UV-Vis spectra were recorded on Cary 50 spectrophotometer. UV-vis/near-IR spectra was recorded on Perkin-Elmer Lambda 1050 UV/vis/NIR spectrophotometer in Prof. YuHuang Wang's lab at University of Maryland. 1,3-Propanedithiol and 1,4-butanedithiol were obtained from Acros and were stored over activated 4 Å molecular sieves under nitrogen.

***In situ* UV-vis/near IR spectral analysis of $[Cu_2S_2]^+$.** $\mathbf{3}^+$OTf and $\mathbf{4}^+$OTf were generated at -40 °C or RT in CH_2Cl_2 followed by immediate analysis. Solutions of these cations were made *in situ* immediately before use.

$[\{[Cl_2IPr]Cu\}_2(\mu\text{-}S(CH_2)_3S)]^+OTf$ ($\mathbf{3}^+OTf$): A solution of $[Cp_2Fe]OTf$ (0.3 mL, 1 mM) was added to a solution of **3** (0.30 mL, 1 mM, in 2.4 mL CH_2Cl_2) with syringe to give 0.1 mM concentrations of $[Cp_2Fe]OTf$ and **3** prior to reaction. The colorless solution immediately turned to green. UV-vis/near IR (CH_2Cl_2, nm, ($cm^{-1}M^{-1}$, RT): 610 (1260), 1150 (1180). The values of molar absorptivity may be considered as lower limits due to the instability of $\mathbf{3}^+$. Titration of **3** with varying equiv. $[Cp_2Fe]OTf$ at -20 °C (see below) did not reliably give the molar absorptivity of **3** due to the instability of cationic $\mathbf{3}^+$.

$[\{[Cl_2IPr]Cu\}_2(\mu\text{-}S(CH_2)_4S)]^+OTf$ ($\mathbf{4}^+OTf$): A similar procedure was used to generate $\mathbf{4}^+$OTf *in situ* as described for the preparation of $\mathbf{3}^+$OTf.

Neutral **4** was titrated via UV-vis spectroscopy with increasing equivalents of $[Cp_2Fe]OTf$ to establish the stoichiometry of this reaction as well as the molar absorptivity of $\mathbf{4}^+$ (Fig. S1). **4** (0.057 g, 0.050 mmol) was dissolved in 2 mL CH_2Cl_2. The solution was analytically transferred to a 10.00 mL volumetric flask and diluted to 10.00 mL with CH_2Cl_2 to give a 5 mM solution of **4**. This solution of **4** in CH_2Cl_2 solution (0.600 mL, 5 mM, 3 μmol) along with various amount of CH_2Cl_2 were placed in a quartz cuvette with a screw top and septum. The cuvette was cooled to

-20 °C in the UV-vis spectrometer. Five solutions of $\mathbf{4}^{+}$OTf at varying concentrations were made with various concentrations of $[Cp_2Fe]$OTf corresponding to the addition of 0.25, 0.50, 0.75, 1.00, and 1.25 equiv. $[Cp_2Fe]$OTf to **4** (Table S1). The maximum value of Abs(645 nm) is obtained after addition of 1.00 equiv. $[Cp_2Fe]$OTf to **4**; addition of excess oxidant results in a lower absorbance at 645 nm suggesting some decay of $\mathbf{4}^{+}$**.** UV-vis/near-IR for $\mathbf{4}^{+}$ (CH_2Cl_2, nm, ($cm^{-1}M^{-1}$, -40 °C): 645 (3050), 1160 (2960).

Table 1 Reaction of **4** and $[Cp_2Fe](OTf)^{-}$ to form $\mathbf{4}^{+}(OTf)^{-}$ *in situ*.

$\mathbf{4}^{+}$OTf	**4** (5 mM)	$[Cp_2Fe]^{+}(OTf)^{-}$ (5 mM)	CH_2Cl_2
0.25 mM	0.6 mL	0.15 mL	2.25 mL
0.50 mM	0.6 mL	0.30 mL	2.10 mL
0.75 mM	0.6 mL	0.45 mL	1.95 mL
1.00 mM	0.6 mL	0.60 mL	1.80 mL
1.00 mM	0.6 mL	0.75 mL	1.65 mL

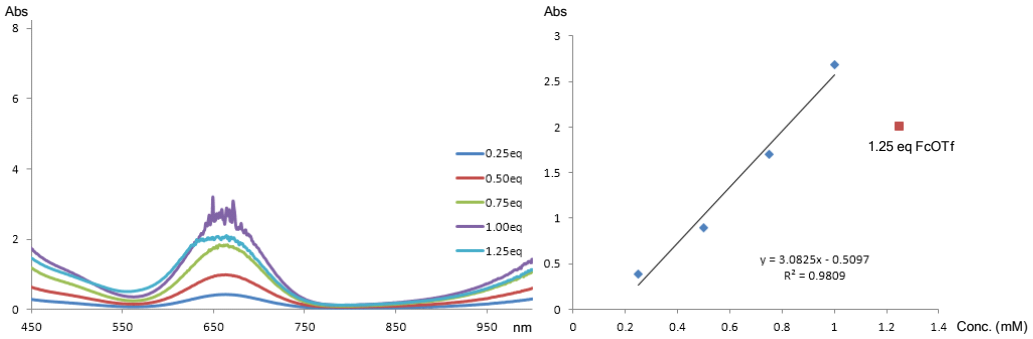

Figure S1. Titration of **4** (1 mM) with 0.25, 0.50, 0.75, 1.00 and 1.25 equiv. $[Cp_2Fe]^{+}(OTf)^{-}$ in CH_2Cl_2 at -20 °C.

Kinetics of $[\{[Cl_2IPr]Cu\}_2(\mu\text{-}S(CH_2)_4S)]^{+}(OTf)^{-}$ ($\mathbf{4}^{+}$OTf) decomposition.

4 (0.057 g, 0.050 mmol) was dissolved in 2 mL CH_2Cl_2. The solution was analytically transferred to a 10.00 mL volumetric flask and diluted to 10.00 mL with CH_2Cl_2 to give a 5 mM solution of **4**. This solution of **4** in CH_2Cl_2 solution (0.600 mL, 5 mM, 3 μmol) along with 2.1 mL CH_2Cl_2 were placed in a quartz cuvette with a screw top and septum. The cuvette was cooled to -20 °C in the UV-vis spectrometer. A CH_2Cl_2 solution of $[Cp_2Fe]^{+}$OTf (0.3 mL, 10 mM) was then syringed into the cuvette. Maintaining the temperature at -20 °C, scans were taken every 5 minutes. Two bands with λ_{max} = 645 and 1150 nm corresponding to $[\{[Cl_2IPr]Cu\}_2(\mu\text{-}S(CH_2)_4S)]$OTf reached maximum immediately after the addition of $[Cp_2Fe]$OTf and slowly lost intensity over the course of 8 h. A plot of $\ln[A_{645}]$ vs. time reveals a straight line pointing to a first-order decomposition of $\mathbf{4}^{+}$ under these conditions for which the first order rate constant $k = 6.8(2) \times 10^{-5}\ s^{-1}$ may be obtained with $t_{1/2}$ = 4.1 h.

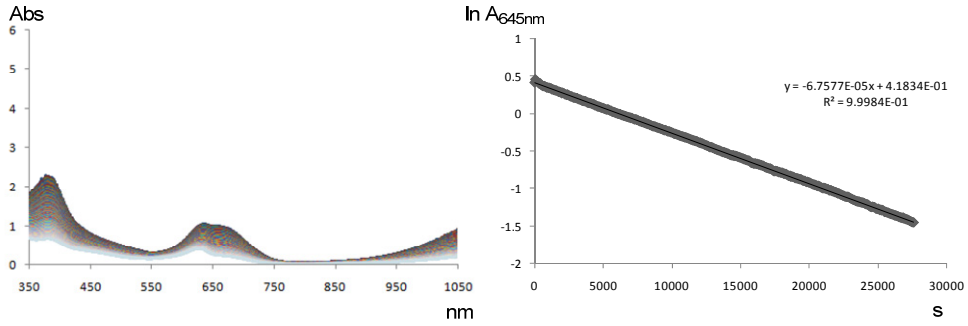

Figure S2. (a) Decomposition of **4**$^{+}$OTf followed by UV-vis spectroscopy in CH_2Cl_2 at -20 °C (5 min/scan, 8h total time interval), (b) plot of ln[A_{645}] vs. time(s)).

Cyclic Voltammetry Details. Cyclic voltammetry measurements were done in an N_2 atmosphere using BASi Epsilon Electrochemistry System with three electrodes (Pseudo-reference: Ag wire; Working: Glassy Carbon; Auxillary: Platinum). The $[Bu_4N]PF_6$ electrolyte was recrystallized from ethanol and thoroughly dried prior to use.

General Reference for cyclic voltammetry details.

(a) Connelly, N. G.; Geiger, W. E. *Chem. Rev.* **1996**, *96*, 877-910.

***In situ* cyclic voltammetry analysis of $[Cu_2S_2]^+$ (Fig 9a and 9b in manuscript).** $\mathbf{3}^+BF_4$ and $\mathbf{4}^+BF_4$ were generated *in situ* at low temperature in CH_2Cl_2 followed by immediate CV analysis.

3 (0.012 g, 0.010 mmol) and the electrolyte $[Bu_4N]PF_6$ (0.775 g, 2.0 mmol) were dissolved in 4 mL CH_2Cl_2. The solution was transferred to a standard three-electrode electrochemical cell. Due to the instability of $\mathbf{3}^+$ at room temperature, the solution of **3** was cooled at -40 °C for 5 minutes inside the cell. A cold CH_2Cl_2 solution of $[Cp_2Fe]^+BF_4$ (1 mL, 1 mM) was quickly injected into the cell, and a scan was taken immediately after the color of the resulted solution changed into dark green indicating the formation of $\mathbf{3}^+$. A similar procedure was used to generate $\mathbf{4}^+BF_4$ *in situ* for CV analysis.

Figure S3. Cyclic voltammogram of $\{[Cl_2IPr]Cu\}_2(\mu\text{-}S(CH_2)_3S)$ (**3**) and ferrocene standards in THF at 2.0 mM and 1.0 mM concentrations, respectively. Horizontal axis in volts.

Electrolyte: 0.40 M NBu_4PF_6 in THF. Scan rate 50 mV/s and 200 mV/s

Ferrocene: 0.81 V *vs.* NHE[a]

Ferrocene Wave: Epa - Epc = 0.12 V

$E_{ox(closed)}$ = -0.51 V *vs.* Fc;

$E_{ox(open)}$ = +0.63 V *vs.* Fc;

$E_{ox(closed)}$ = 0.30 *vs.* NHE;

$E_{ox(open)}$ = 1.44 V *vs.* NHE;

Epa - Epc = 0.15 V.

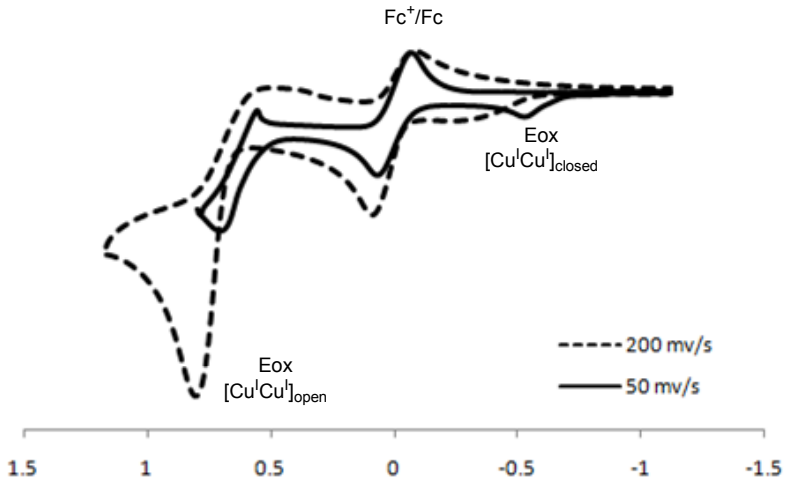

Figure S4. Cyclic voltammogram of $\{[Cl_2IPr]Cu\}_2(\mu\text{-}S(CH_2)_4S)$ (**4**) and ferrocene standards in THF at 2.0 mM and 1.0 mM concentrations, respectively. Horizontal axis in volts.

Electrolyte: 0.40 M NBu_4PF_6 in THF. Scan rate 50 mV/s and 200 mV/s
Ferrocene: 0.81 V *vs.* NHE[a]
Ferrocene Wave: Epa – Epc = 0.13 V
$E_{ox(closed)}$ = -0.43 V *vs.* Fc;
$E_{ox(open)}$ = 0.95 V *vs.* Fc;
$E_{ox(closed)}$ = 0.38V *vs.* NHE;
$E_{ox(open)}$ = 1.76 V *vs.* NHE;

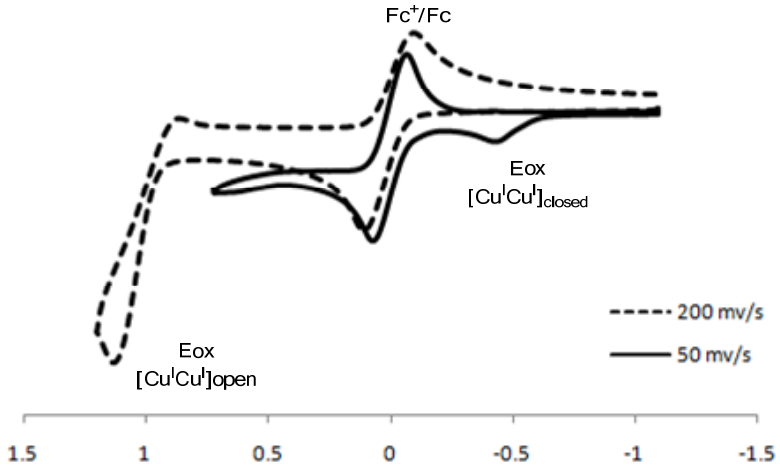

Figure S5. Cyclic voltammogram of $[Cl_2IPr]Cu\text{-}SCH_2CH_2Ph$ (**5**) and ferrocene standards in THF at 2.0 mM and 1.0 mM concentrations, respectively. Horizontal axis in volts.

Electrolyte: 0.40 M NBu_4PF_6 in THF. Scan rate 50 mV/s
Ferrocene: 0.81 V *vs.* NHE[a]
Ferrocene Wave: Epa - Epc = 0.12 V
$E_{ox(mononuclear)}$ = 1.18 V *vs.* Fc ;
$E_{ox(mononuclear)}$ = 1.99 V *vs.* NHE;

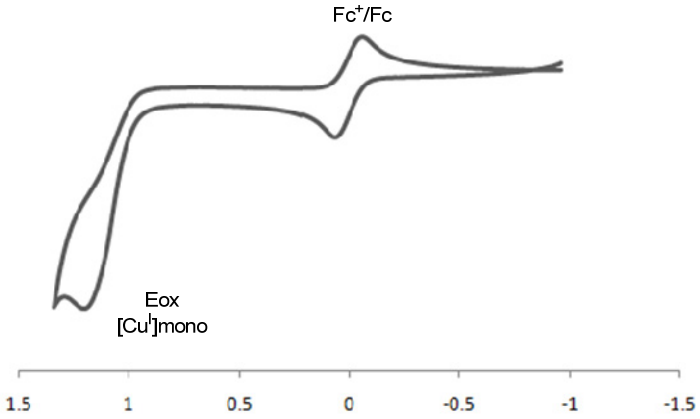

Figure S6. Cyclic voltammogram of $\{[Cl_2IPr]Cu\}_2(\mu\text{-}S(CH_2)_3S)$ (**3**) in CH_2Cl_2 at 2.0 mM concentrations, respectively. Horizontal axis in volts.

Electrolyte: 0.40 M NBu_4PF_6 in CH_2Cl_2. Scan rate 50 mV/s, 100 mV/s, 200 mV/s, 400 mV/s.
Ferrocene: 0.81 V *vs.* NHE[a]
Epa - Epc = 0.10 V;
$E_{ox(closed)}$ = -0.55V *vs.* Fc;
$E_{ox(open)}$ = 0.78 V *vs.* Fc;
$E_{ox(closed)}$ = 0.26 V *vs.* NHE;
$E_{ox(open)}$ = 1.59 V *vs.* NHE.

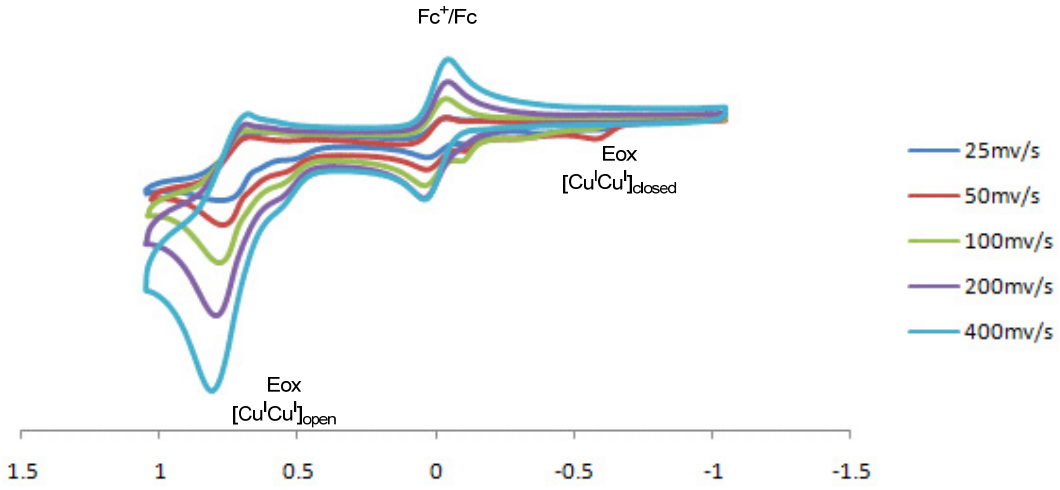

Figure S7. Cyclic voltammogram of {[Cl_2IPr]Cu}$_2$(μ-S$(CH_2)_4$S) (**4**) and ferrocene standards in CH_2Cl_2 at 2.0 mM concentrations, respectively. Horizontal axis in volts.

Electrolyte: 0.40 M NBu_4PF_6 in CH_2Cl_2. Scan rate 50 mV/s,

$E_{ox(closed)}$ = -0.39 V *vs.* Fc;
$E_{1/2(closed)}$ = -0.42 V *vs.* Fc;
$E_{1/2(closed)}$ = 0.39 V *vs.* NHE;

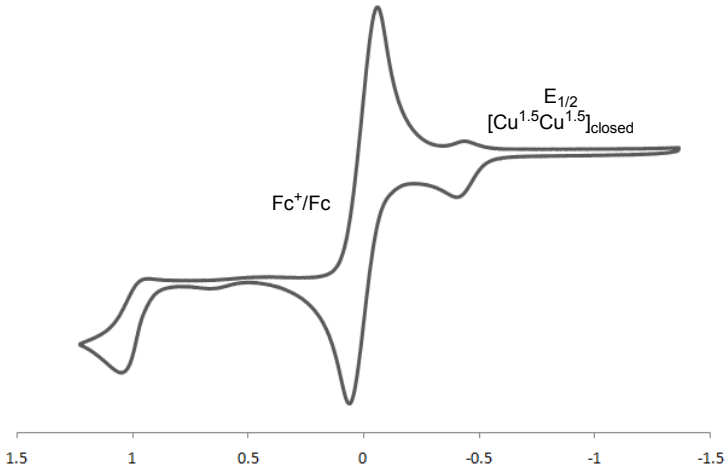

Figure S8. Cyclic voltammogram of [Cl_2IPr]Cu-SCH_2CH_2Ph (**5**) and ferrocene standards in CH_2Cl_2 at 2.0 mM and 1.0 mM concentrations, respectively. Horizontal axis in volts.

Electrolyte: 0.40 M NBu_4PF_6 in CH_2Cl_2. Scan rate 50 mV/s
Ferrocene: 0.81 V *vs.* NHE[a]
Ferrocene Wave: Epa - Epc = 0.12 V
$E_{ox(mononuclear)}$ = 1.10 V *vs.* Fc ;
$E_{ox(mononuclear)}$ = 1.91 V *vs.* NHE;

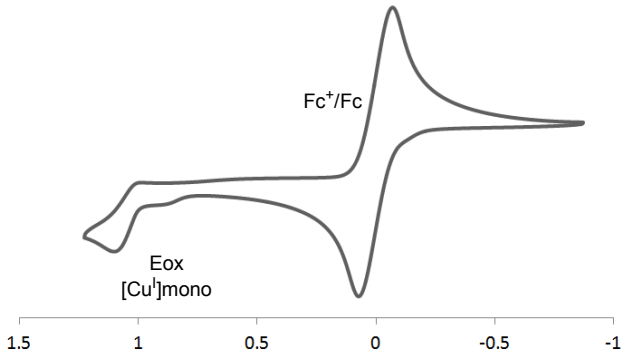

DFT Calculation Details

The DFT calculations employed the Becke-Perdew exchange correlation functional [1] using the Amsterdam Density Functional suite of programs (ADF 2007.01) [2]. Slater-type orbital (STO) basis sets employed for H, C, and N atoms were of triple-quality augmented with two polarization functions (ZORA/TZ2P) while an improved triple-ζ basis set with two polarization functions (ZORA/TZ2P+) was employed for the Cu atom. Scalar relativistic effects were included by virtue of the zero order regular approximation (ZORA) [3]. The 1s electrons of C and N as well as the 1s – 2p electrons of Cu were treated as frozen core. The VWN (Vosko, Wilk, and Nusair) functional was used for LDA (local density approximation) [4]. Mostly default convergence (E = 1×10^{-4} hartree (default = 1×10^{-3} hartree), max. gradient = 1×10^{-2} hartree / Å, max. Cartesian step = 1×10^{-2} Å) and integration (4 significant digits) parameters were employed for geometry optimizations.

Experimental X-ray coordinates for **3** were used as the starting point for the geometry optimization of these species in unrestricted (S = 1/2) calculations specifying 1 unpaired electron (spin α – spin β). ADFview [2a] was used to prepare the three-dimensional representations of the structures as well as to render the Kohn-Sham MOs which appear in Figures S10, S12, S14, S16 as well as the net spin density contour plots in Figures S10, S14. Converged DFT atomic coordinates for $\mathbf{3}^{+}$ and $\mathbf{4}^{+}$ are collected in Tables S3 and S4, respectively.

[1] (a) Becke, A. *Phys. Rev. A* **1988**, *38*, 3098. (b) Perdew, J. P. *Phys. Rev. B* **1986**, *34*, 7406. (c) Perdew, J. P. *Phys. Rev. B* **1986**, *33*, 8822.
[2] (a) http://www.scm.com – last accessed June 24, 2012. (b) te Velde, G.; Bickelhaupt, F.M.; Baerends, E. J.; Fonseca Guerra, C.; Van Gisbergen, S. J. A.; Snijders, J. G.; Ziegler, T. *J. Comput. Chem.* **2001**, *22*, 931. (c) Fonseca Guerra, C.; Snijders, J. G.; te Velde, G.; Baerends, E. J.; Acc., T. C. *Theor. Chem. Acc.* **1998**, *99*, 391.
[3] (a) Snijders, J. G.; Baerends, E. J.; Ros, P. *Mol. Phys.* **1979**, *38*, 1909. (b) Ziegler, T.; Tschinke, V.; Baerends, E. J.; Snijders, J. G.; Ravenek, W. K. *J. Phys. Chem.* **1989**, *93*, 3050. (c) van Lenthe, E.; Baerends, E. J.; Snijders, J. G. *J. Chem. Phys.* **1993**, *99*, 4597.
[4] Vosko, S. H.; Wilk, L.; Nusair, M. *Can. J. Phys.* **1980**, *58*, 1200.

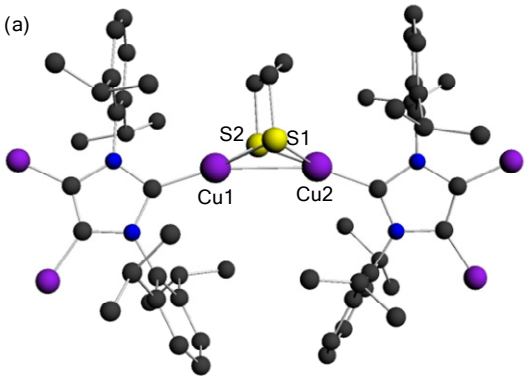

{[Cl_2IPr]Cu}$_2$(μ-S$(CH_2)_3$S) (**3**)

Cu1-Cu2	2.974 Å
S1-S2	3.361 Å
Cu1-S1	2.328 Å
Cu1-S2	2.368 Å
Cu2-S1	2.371 Å
Cu2-S2	2.326 Å

Figure S9. DFT structure for {[Cl_2IPr]Cu}$_2$(μ-S$(CH_2)_3$S) (**3**) along with selected bond distances.

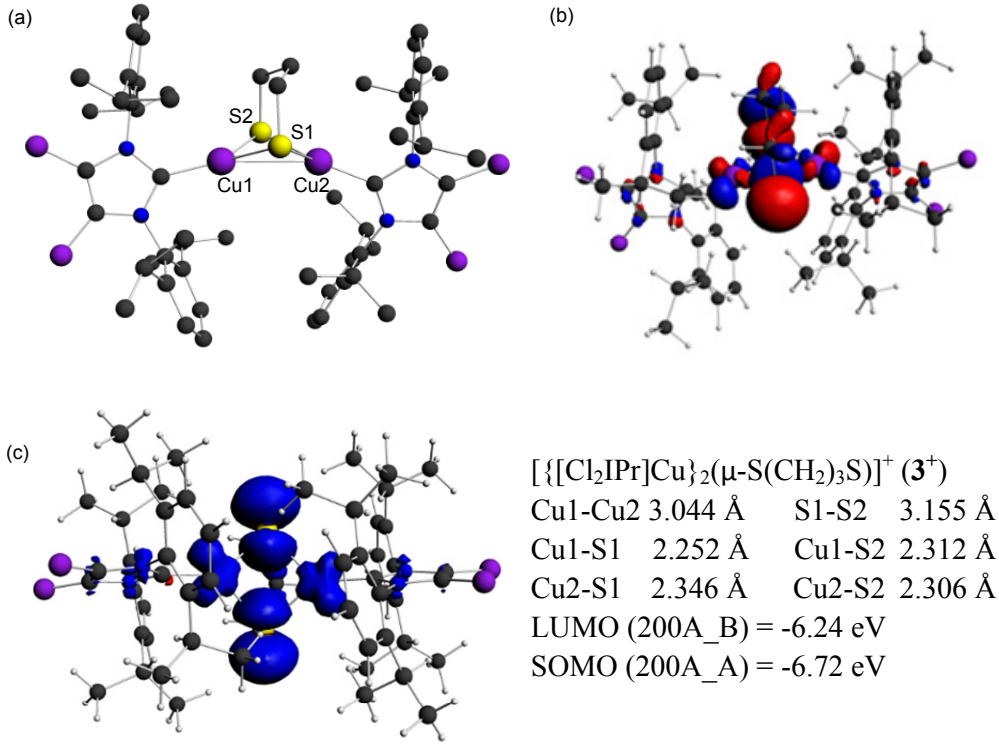

[{[Cl_2IPr]Cu}$_2$(μ-S$(CH_2)_3$S)]$^+$ (**3**$^+$)

Cu1-Cu2	3.044 Å	S1-S2	3.155 Å
Cu1-S1	2.252 Å	Cu1-S2	2.312 Å
Cu2-S1	2.346 Å	Cu2-S2	2.306 Å

LUMO (200A_B) = -6.24 eV

SOMO (200A_A) = -6.72 eV

Figure S10. (a) DFT structure, (b) contour plot of SOMO (spin α; upper right) (c) spin density plot (blue = excess spin α, red = excess spin β (0.001 isospin value)) for [{[Cl_2IPr]Cu}$_2$(μ-S$(CH_2)_3$S)]$^+$ (**3**$^+$) with selected bond distances from the optimized DFT structure. DFT electron spin densities predicted: Cu1 0.13 e^-; Cu2 0.15 e^-; S1 0.33 e^-; S2 0.33 e^-.

Table S2. Observed vs. TD-DFT calculated low energy electronic transitions for $\mathbf{3}^{+}$.

Optical Transition (nm ($M^{-1}cm^{-1}$))	Calculated Transition (nm)	Oscillator Strength	Principal Components
610 (1260)	653	0.023	191a -> 200a (66.9%) 193a -> 200a (18.0%) 192a -> 200a (11.2%)
1150 (1180)	1140	0.042	199a -> 200a (72.0%) 198a -> 200a (26.3%)

Figure S11. Observed (black) vs. TD-DFT calculated (red) UV-vis/near IR spectra for $\mathbf{3}^{+}$.

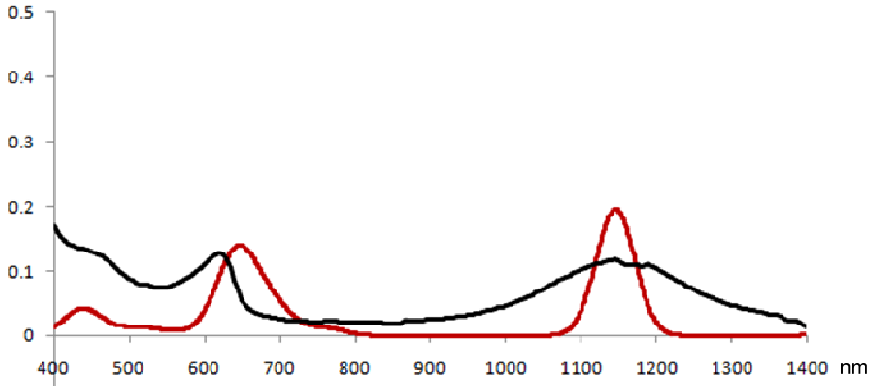

Figure S12. Contour plots of spin β Kohn-Sham MOs involved in key optical and near IR transitions for $\mathbf{3}^{+}$: (a) 191a, (b), 193a (c) 199a, (d) 200a.

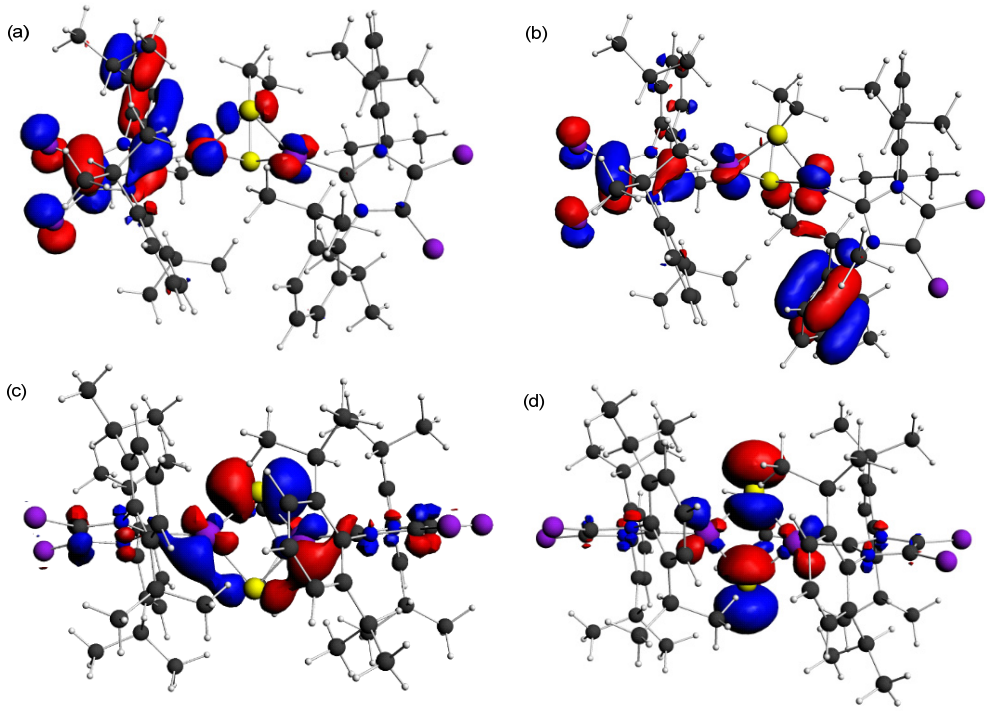

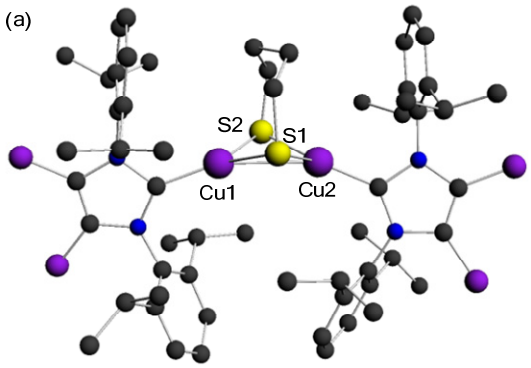

{[Cl_2IPr]Cu}$_2$(μ-S$(CH_2)_4$S) (**4**)

Cu1-Cu2	2.903 Å
S1-S2	3.526 Å
Cu1-S1	2.410 Å
Cu1-S2	2.309 Å
Cu2-S1	2.310 Å
Cu2-S2	2.414 Å

Figure S13. DFT structure for {[Cl_2IPr]Cu}$_2$(μ-S$(CH_2)_4$S) (**4**) along with selected bond distances.

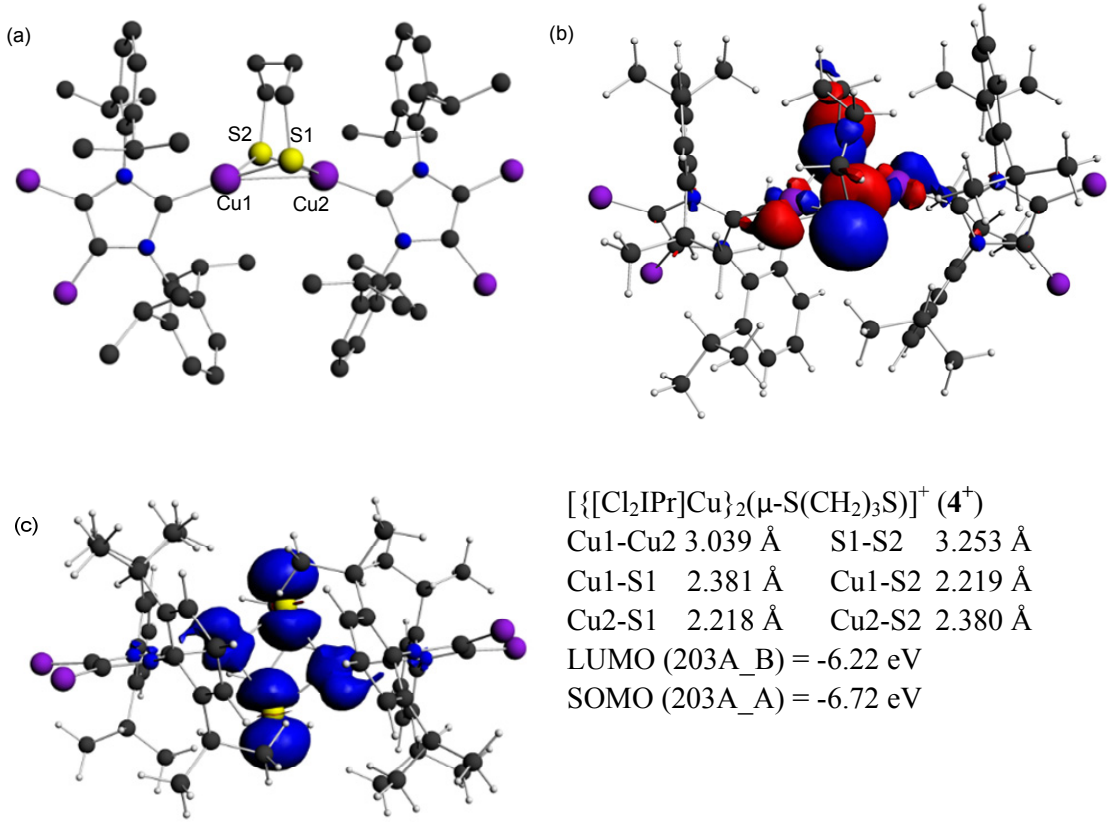

[{[Cl_2IPr]Cu}$_2$(μ-S$(CH_2)_3$S)]$^+$ (**4**$^+$)

Cu1-Cu2	3.039 Å	S1-S2	3.253 Å
Cu1-S1	2.381 Å	Cu1-S2	2.219 Å
Cu2-S1	2.218 Å	Cu2-S2	2.380 Å

LUMO (203A_B) = -6.22 eV
SOMO (203A_A) = -6.72 eV

Figure S14. DFT structure (left), contour plot of SOMO (spin α; middle), and spin density plot (right; blue = excess spin α, red = excess spin β (0.001 isospin value)) for [{[Cl_2IPr]Cu}$_2$(μ-S$(CH_2)_4$S)]$^+$ (**4**$^+$) with selected bond distances and angles from the optimized DFT structure. DFT electron spin densities predicted: Cu1 0.15 e^-; Cu2 0.15 e^-; S1 0.32 e^-; S2 0.32 e^-.

Table S3. Observed vs. TD-DFT calculated low energy electronic transitions for $\mathbf{4}^{+}$.

Optical Transition (nm ($M^{-1}cm^{-1}$))	Calculated Transition (nm)	Oscillator Strength	Principal Components
645 (3050)	590	0.015	195a -> 203a (82.0%) 193a -> 203a (13.0%)
1150 (2960)	1073	0.034	202a -> 203a (94.6%) 200a -> 203a (2.2%)

Figure S15. Observed (black) vs. TD-DFT calculated (red) UV-vis/near IR spectra for $\mathbf{4}^{+}$.

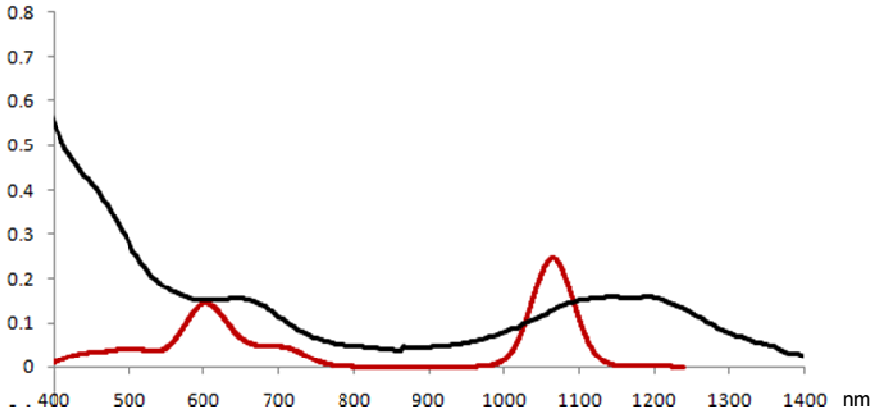

Figure S16. Contour plots of spin β Kohn-Sham MOs involved in key optical and nearIR transitions for $\mathbf{4}^{+}$ (a) 193a, (b) 195a, (c) 202a, (d) 203a.

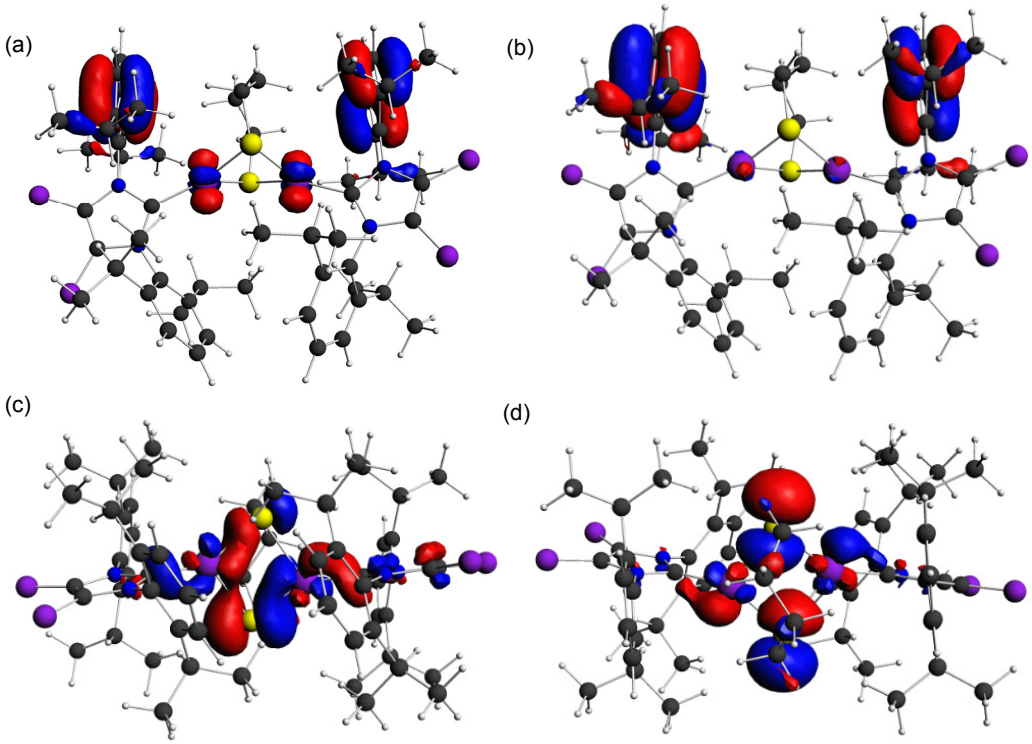

Table S4. DFT optimized coordinates for [{[Cl_2IPr]Cu}$_2$(μ-S(CH_2)$_3$S)]$^+$ (**3**$^+$)

	Atom	X	Y	Z	(Angstrom)
1	Cu	1.14313507	1.04323588	-0.16232884	
2	Cu	-1.86067889	0.98746576	0.32531626	
3	S	-0.19331811	1.7550081	1.62930328	
4	S	-0.62262257	1.69299027	-1.49572907	
5	N	4.05480028	1.22746123	-0.12355826	
6	N	-4.72739275	1.25545128	0.41336756	
7	C	2.95041857	0.40023958	-0.27713435	
8	C	-3.65694904	0.44813788	0.5188148	
9	N	3.45575443	-0.84281821	-0.53348515	
10	N	-4.1926138	-0.76449488	0.7624108	
11	C	4.00395539	3.5129399	-0.98768627	
12	C	-4.71965604	3.56876455	1.18357275	
13	C	2.7290377	-2.05199777	-0.780117	
14	C	-3.41131451	-1.9975257	0.93608999	
15	C	2.15365379	-2.70344817	0.34478616	
16	C	-2.86537844	-2.6593434	-0.20136289	
17	C	5.20987663	0.51021723	-0.32290598	
18	C	-5.90636435	0.53187374	0.52830256	
19	Cl	6.78927198	1.2055144	-0.35164768	
20	Cl	-7.40317209	1.20346761	0.45838941	
21	C	3.95481544	2.67363446	0.13063146	
22	C	-4.66082903	2.66945648	0.15673004	
23	C	3.85304598	3.0961228	1.46718926	
24	C	-4.55435692	3.11710348	-1.2478095	
25	C	2.22281928	-2.15636311	1.73935729	
26	C	-2.93267287	-2.12665447	-1.61781361	
27	H	2.72616077	-1.10190075	1.6865099	
28	H	-3.35458365	-1.21575903	-1.48982324	
29	C	4.07859937	3.07181149	-2.43272371	
30	C	-4.8291496	3.03319602	2.57852322	
31	H	4.28251367	1.99512426	-2.43835095	
32	H	-5.03413873	1.96369653	2.50203253	
33	C	4.83477837	-0.8096185	-0.53566091	
34	C	-5.54484451	-0.75048244	0.75861006	
35	Cl	5.82771068	-2.14402639	-0.75816314	
36	Cl	-6.51929953	-2.09346928	0.98980452	
37	C	3.86785821	2.13951074	2.62591732	
38	C	-4.58461216	2.11313454	-2.47576215	
39	H	3.51837086	1.1487291	2.25415571	
40	H	-4.17979969	1.11470747	-2.10839165	
41	C	3.81343881	5.35189469	0.62825919	

42	C	-4.51453845	5.43449879	-0.34650489
43	H	3.74515064	6.40284516	0.80581566
44	H	-4.39199805	6.44763336	-0.56238053
45	C	1.99754087	-3.77413993	-2.28950467
46	C	-2.6805369	-3.75381313	2.39621039
47	H	1.86628192	-4.138999	-3.26027454
48	H	-2.60703183	-4.28523163	3.42895195
49	C	3.94583956	4.8931267	-0.7133029
50	C	-4.6078841	4.9168753	0.91508374
51	H	3.96428092	5.594638	-1.54573994
52	H	-4.56559079	5.58594194	1.69617605
53	C	1.52165149	-3.96881391	0.14500859
54	C	-2.24164791	-3.9361511	0.02044972
55	H	1.06704606	-4.45440895	1.02974898
56	H	-1.8470318	-4.47536229	-0.79409029
57	C	1.4806162	-4.49902749	-1.17368842
58	C	-2.12804646	-4.49080633	1.31488425
59	H	0.97253001	-5.43437728	-1.31620905
60	H	-1.67321241	-5.43630159	1.52739436
61	C	3.81494418	4.45485897	1.72456888
62	C	-4.4873678	4.58001164	-1.43284738
63	H	3.74764853	4.77828757	2.72855155
64	H	-4.40406652	5.01095	-2.47437701
65	C	3.20900344	-1.77900769	-3.29374264
66	C	-3.94104675	-1.74497149	3.45525892
67	H	4.08570137	-1.23321304	-2.94365995
68	H	-4.8178636	-1.15094386	3.19299811
69	C	2.67786841	-2.56991096	-2.0785016
70	C	-3.32177724	-2.50800459	2.23245822
71	C	2.10933691	-0.78395077	-3.78917289
72	C	-2.84898932	-0.70566158	3.95890954
73	H	1.28427567	-1.28302686	-4.1559363
74	H	-1.91293397	-1.25372871	4.30515233
75	H	2.40814534	-0.20237047	-4.60643489
76	H	-3.27767806	-0.11495466	4.78229163
77	H	1.8001199	-0.11874516	-2.97967777
78	H	-2.55483071	-0.03332751	3.22753494
79	C	0.81470022	-2.03295647	2.48784854
80	C	-1.5080223	-2.03536723	-2.21772223
81	H	0.11961273	-1.44571216	1.94689203
82	H	-0.89660242	-1.4111174	-1.64483059
83	H	0.89760824	-1.61280583	3.49179486
84	H	-1.60298051	-1.65261469	-3.174146
85	H	0.26735209	-2.93847025	2.58555173

86	H	-1.1219686	-2.96679584	-2.34732178
87	C	3.64643778	-2.70261071	-4.45162355
88	C	-4.39757478	-2.68488279	4.5590049
89	H	4.32890238	-3.42676612	-4.08766632
90	H	-5.01437598	-3.38271601	4.19974497
91	H	4.0872763	-2.09884427	-5.19110067
92	H	-4.90670523	-2.10013139	5.29372405
93	H	2.82533981	-3.18254647	-4.84696198
94	H	-3.55286807	-3.19551158	5.01908177
95	C	2.74135727	3.27791547	-3.1691356
96	C	-3.45179459	3.25184115	3.36027316
97	H	1.9406165	2.79187231	-2.67119098
98	H	-2.65135679	2.7089112	2.9054873
99	H	2.81327592	2.91369825	-4.19394553
100	H	-3.52607423	2.90587433	4.45757663
101	H	2.44495778	4.30455952	-3.21871758
102	H	-3.14973057	4.30476513	3.39414513
103	C	3.19473267	-3.05554909	2.61816442
104	C	-3.87126635	-3.06968412	-2.46845659
105	H	3.30848742	-2.70263795	3.75684451
106	H	-4.00573487	-2.67111487	-3.41722143
107	H	4.24874293	-3.17281454	2.21495277
108	H	-4.80322565	-3.17222547	-1.97822923
109	H	2.79129701	-4.15238731	2.69899359
110	H	-3.47486301	-4.00768446	-2.61573799
111	C	2.96488233	2.55894853	3.78034928
112	C	-3.63270561	2.54032548	-3.6645968
113	H	3.31707036	3.46118306	4.22416868
114	H	-3.96492612	3.49405728	-4.23028405
115	H	2.98360147	1.76866228	4.50141058
116	H	-3.63487366	1.739954	-4.41135187
117	H	1.9619668	2.6742149	3.46923665
118	H	-2.57442381	2.71820524	-3.38674268
119	C	5.34288613	1.92429885	3.13067663
120	C	-6.1003518	1.90175104	-2.95755028
121	H	5.97152565	1.59713888	2.30963923
122	H	-6.75284214	1.52973295	-2.22478844
123	H	5.38098554	1.12330162	3.92426789
124	H	-6.14384374	1.17777829	-3.77052167
125	H	5.7742587	2.85336472	3.52012551
126	H	-6.60180206	2.8054733	-3.32597123
127	C	5.23652326	3.7586236	-3.19686383
128	C	-5.96144654	3.72762241	3.33820408
129	H	5.11465935	4.8020209	-3.32612545

130	H	-5.80230459	4.81794622	3.47339702
131	H	5.31140715	3.35874815	-4.20018334
132	H	-6.0405934	3.23486766	4.31773451
133	H	6.18213335	3.60529835	-2.69807192
134	H	-6.88580305	3.59680195	2.81204176
135	C	0.08576503	4.04680699	-0.02542258
136	H	1.1920198	3.82806011	-0.22186924
137	H	0.04761395	5.1398498	-0.02235097
138	C	-0.36176757	3.57102672	1.38760251
139	H	-1.30188101	3.85696161	1.65451943
140	H	0.28877237	3.99381439	2.12435943
141	C	-0.73531713	3.54697084	-1.23688122
142	H	-1.75748108	3.81857761	-1.12398548
143	H	-0.39209516	3.95724003	-2.16906193

Table S5. DFT optimized coordinates for $[\{[Cl_2IPr]Cu\}_2(\mu\text{-}S(CH_2)_4S)]^+$ (**4**$^+$)

	Atom	X	Y	Z	(Angstrom)
1	Cu	1.80461242	-0.89664898	-1.60027392	
2	Cl	3.85623284	-1.9330157	-6.75859775	
3	Cl	3.97635131	1.53978325	-6.33685148	
4	S	2.00748664	-1.37015798	0.55724548	
5	N	2.8521658	-1.53028751	-4.23836454	
6	C	0.58778852	2.27354526	-3.53846843	
7	H	0.61271021	1.18399349	-3.66787693	
8	C	2.61443373	-0.53963894	-3.31711168	
9	C	3.45752764	0.34869709	-5.23585245	
10	C	3.13530993	1.93015039	-3.33508681	
11	C	3.38014921	-1.00282181	-5.41352422	
12	C	6.1050967	-3.40910548	-3.56984706	
13	H	6.27881342	-4.48298289	-3.4110781	
14	H	7.02586059	-2.87436398	-3.29772178	
15	H	5.92025702	-3.25338668	-4.64076524	
16	N	3.00468327	0.61827588	-3.94218842	
17	C	3.40087208	-4.93121367	-2.84166909	
18	H	4.12163194	-5.46576912	-2.22328473	
19	C	4.56830776	3.67595822	-2.52080632	
20	H	5.55693297	4.04886782	-2.25574881	
21	C	1.99465468	2.74202332	-3.1925793	
22	C	5.67041396	1.47387918	-3.08879172	
23	H	5.42696028	0.61148279	-3.72294345	
24	C	4.92674941	-2.91130975	-2.70634897	
25	H	4.82426772	-1.83181513	-2.87286555	
26	C	0.08969146	2.8974719	-4.85614898	
27	H	0.03392424	3.99238898	-4.77087973	

28	H	-0.91772512	2.52590616	-5.09165096
29	H	0.75133822	2.65830635	-5.69903511
30	C	2.66517092	-2.93771238	-3.95539914
31	C	3.46419113	4.51419863	-2.40252067
32	H	3.59647505	5.53892611	-2.05834935
33	C	0.48549868	-3.64260295	-6.79276026
34	H	1.47475591	-3.69899662	-7.26293997
35	H	-0.18825542	-3.10202673	-7.47139602
36	H	0.10062342	-4.66649314	-6.68786097
37	C	0.54158999	-2.92805915	-5.42857451
38	H	0.87355049	-1.89679921	-5.60507823
39	C	4.43573037	2.36497355	-2.99299566
40	C	3.63070803	-3.5842261	-3.15115917
41	C	1.37578468	-4.94888403	-4.15450219
42	H	0.5168425	-5.49266281	-4.54773941
43	C	-0.86589301	-2.8494539	-4.81089106
44	H	-1.25026898	-3.85086467	-4.56928205
45	H	-1.56445417	-2.38750638	-5.52225593
46	H	-0.86211406	-2.24327907	-3.89596
47	C	5.23655856	-3.10259506	-1.21308847
48	H	4.45083159	-2.66961348	-0.57990727
49	H	6.18085797	-2.60000162	-0.96393023
50	H	5.35384489	-4.16275829	-0.95040533
51	C	2.28361182	-5.60481774	-3.3289992
52	H	2.12950279	-6.65302706	-3.07565351
53	C	2.19449661	4.04641625	-2.72135683
54	H	1.33506647	4.70534633	-2.6076851
55	C	6.86952153	2.18647997	-3.73931802
56	H	7.25521593	2.99405144	-3.10210171
57	H	6.60552382	2.61803393	-4.71312446
58	H	7.69107853	1.4733471	-3.89069719
59	C	-0.40001556	2.57477977	-2.39994166
60	H	-0.04713809	2.17362669	-1.43967459
61	H	-1.37712604	2.1245433	-2.61797653
62	H	-0.55042946	3.65502865	-2.27266709
63	C	1.54343281	-3.59911498	-4.49393222
64	C	1.76064877	-3.21694888	0.62075352
65	C	6.05754046	0.92375681	-1.70117625
66	H	6.92637515	0.25584721	-1.78760219
67	H	5.23243653	0.36323095	-1.24260017
68	H	6.32965898	1.74247012	-1.02017541
69	C	0.33498424	-3.75745429	0.52406333
70	Cu	-0.05287664	-0.18531625	0.69681349
71	Cl	-2.26993416	0.7817087	5.79441046

72	Cl	-0.51230931	3.68369363	4.93259519
73	S	-0.5624006	-0.8334311	-1.363747
74	N	-1.24326308	0.22962818	3.31232636
75	C	2.70068935	2.11163286	2.27174276
76	H	2.10344093	1.22427717	2.51723966
77	C	-0.52183174	0.79913657	2.29122188
78	C	-0.7313305	2.26001141	4.02405296
79	C	0.35762225	3.14434673	1.96314299
80	C	-1.3892817	1.11662159	4.37532568
81	C	-5.01076782	0.32121271	2.67620291
82	H	-5.73876528	-0.50200087	2.64353456
83	H	-5.5005328	1.22020382	2.27648994
84	H	-4.75889903	0.50560253	3.72875114
85	N	-0.22170219	2.06186568	2.73859499
86	C	-3.5702311	-2.49792832	2.32705401
87	H	-4.47657785	-2.64024696	1.73892319
88	C	0.06181937	5.24996286	0.84762953
89	H	-0.58077755	6.04837463	0.47821903
90	C	1.7529922	3.19986797	1.78591804
91	C	-2.03417095	4.07983438	1.63466581
92	H	-2.27701754	3.31945182	2.38816536
93	C	-3.7608428	-0.01980009	1.83726455
94	H	-3.08918702	0.84691406	1.871496
95	C	3.45468339	2.54408551	3.54389356
96	H	4.08630801	3.42117451	3.3414158
97	H	4.10788945	1.73045738	3.88989225
98	H	2.76727842	2.80484082	4.3592768
99	C	-1.85237685	-1.08098443	3.22108541
100	C	1.44005721	5.34916896	0.68729915
101	H	1.86782527	6.22619303	0.20341637
102	C	-0.35782085	-2.45484678	6.25543736
103	H	-1.21599072	-1.91172856	6.6695788
104	H	0.51053591	-2.27195764	6.90287019
105	H	-0.58379863	-3.52934545	6.29808106
106	C	-0.04161141	-2.00953393	4.81448539
107	H	0.23424482	-0.94769883	4.84636924
108	C	-0.51627814	4.15065327	1.49307693
109	C	-3.02820975	-1.21180575	2.44745829
110	C	-1.85556136	-3.41870305	3.75355701
111	H	-1.42240521	-4.27815341	4.26516069
112	C	1.17811451	-2.77732262	4.27487281
113	H	0.96025829	-3.85057238	4.17734429
114	H	2.02706704	-2.670297	4.96406689
115	H	1.48466796	-2.39112025	3.29452785

116	C	-4.14515852	-0.22769876	0.36338929
117	H	-3.25973124	-0.3923793	-0.26495783
118	H	-4.66200829	0.66524091	-0.0134534
119	H	-4.82932582	-1.07745531	0.23421044
120	C	-2.98760698	-3.59095057	2.96347123
121	H	-3.43029332	-4.58050955	2.85523335
122	C	2.27051324	4.33075232	1.14064584
123	H	3.34654192	4.41114307	0.99509284
124	C	-2.64764105	5.40577911	2.11920145
125	H	-2.55289111	6.19624237	1.36209536
126	H	-2.17142191	5.75991448	3.04216233
127	H	-3.72019168	5.27222395	2.31501153
128	C	3.69702035	1.69996726	1.17503327
129	H	3.18421194	1.43346409	0.24087191
130	H	4.28086273	0.83015826	1.50281881
131	H	4.40380948	2.50916902	0.94728583
132	C	-1.26036135	-2.15889577	3.90893387
133	C	-1.2878897	-2.53185315	-1.11022997
134	C	-2.69040691	3.63501185	0.31222065
135	H	-3.77976532	3.55778489	0.43750294
136	H	-2.30923524	2.66158119	-0.02235611
137	H	-2.49536535	4.36652206	-0.48460746
138	C	-0.32946958	-3.69609852	-0.8633846
139	H	-1.85007509	-2.71098941	-2.03492491
140	H	-2.01035928	-2.45123019	-0.28761475
141	H	0.43605671	-3.72842445	-1.65462515
142	H	-0.93467707	-4.60785501	-0.99269171
143	H	-0.30583608	-3.26957766	1.27516322
144	H	0.4006079	-4.81552415	0.82501755
145	H	2.19671929	-3.50110724	1.58624948
146	H	2.38587337	-3.65101384	-0.170148

X-Band EPR Details.

EPR measurements were performed in quartz tubes with J.Young valves. Spectral simulation was performed using the program QCMP 136 by Prof. Dr. Frank Neese from the Quantum Chemistry Program Exchange as used by Neese *et al.* (*J. Am. Chem. Soc.* 1996, **118**, 8692-8699). The fittings were performed by the "chi by eye" approach. Solution EPR spectra were recorded on a JEOL continuous wave spectrometer JES-FA200 equipped with an X-band Gunn oscillator bridge, a cylindrical mode cavity, and a liquid nitrogen cryostat. For all samples, a modulation frequency of 100 kHz and a time constant of 0.03 s were employed. Spectra were measured in 5 sweeps of 4 min each.

Sample preparation: A solution of $[Cp_2Fe]OTf$ (0.1 mL, 5 mM) was added to a solution of **3** (0.1 mL, 5 mM, in 0.3 mL CH_2Cl_2) by syringe under N_2 atmosphere at -78 °C to give a concentration of $[Cp_2Fe]OTf$ and **3** of 1.0 mM each prior to reaction. After the solution turned green indicating the formation of $\mathbf{3}^+$, the tube was placed in liquid nitrogen to give a frozen glass sample for EPR measurement. A similar procedure was used to generate $[\{[Cl_2IPr]Cu\}_2(\mu\text{-}S(CH_2)_4S)]^+OTf$ ($\mathbf{4}^+OTf$) *in situ* for EPR measurement. Melting of the frozen samples resulted in a bleaching of the EPR signal.

Figure S17. X-band EPR spectrum and simulation for $[\{[Cl_2IPr]Cu\}_2(\mu\text{-}S(CH_2)_3S)]^+$ (**3**$^+$) (frozen dichloromethane glass, 8.902096 GHz, ModWidth = 0.05 mT, Power = 0.998 mW). Simulation was performed using a 2 Cu model: $g_1 = 2.085$, $g_2 = 2.015$, $g_3 = 2.015$ with A_1(2 Cu) = 150 MHz, A_2(2 Cu) = A_3(2 Cu) = 40 MHz. Gaussian lineshape, line broadening $W1 = 17$ mT, $W2 = 17$ mT, $W3 = 17$ mT.

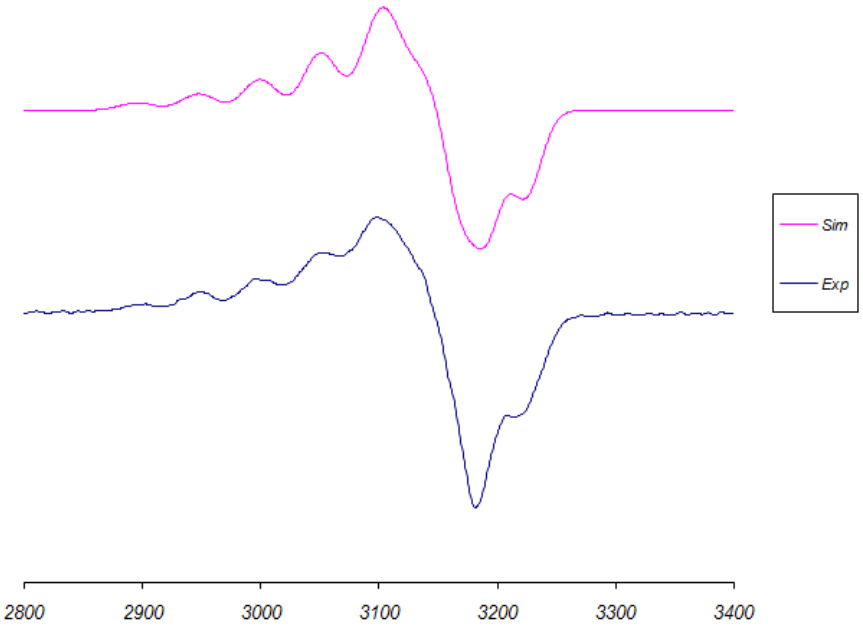

Figure S18. X-band EPR spectrum and simulation for $[\{[Cl_2IPr]Cu\}_2(\mu\text{-}S(CH_2)_4S)]^+$ (**4**$^+$) (frozen dichloromethane glass, 8.905899 GHz, ModWidth = 0.1 mT, Power = 0.998 mW). Simulation was performed using a 2 Cu model: $g_1 = 2.090$, $g_2 = 2.009$, $g_3 = 2.009$ with A_1(2 Cu) = 162 MHz, A_2(2 Cu) = A3(2 Cu) = 40MHz. Gaussian lineshape, line broadening $W1 = 20$ mT, $W2 = 20$ mT, $W3 = 20$ mT.

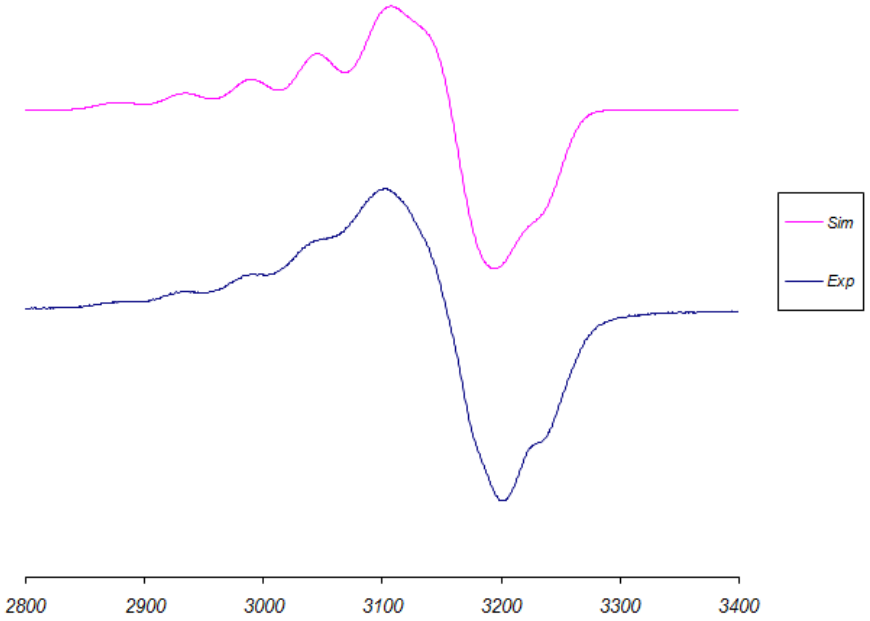

X-ray structure refinement details

Single crystals of each compound **3**, **4** and **5** were mounted under mineral oil on glass fibers and immediately placed in a cold nitrogen stream at 100(2) K on a Bruker SMART CCD system. Either full spheres (triclinic) or hemispheres (monoclinic or higher) of data were collected (0.3° or 0.5° ω-scans; $2\theta_{max} = 56°$; monochromatic Mo Ka radiation, $\lambda = 0.7107$ Å) depending on the crystal system and integrated with the Bruker SAINT program. Structure solutions were performed using the SHELXTL/PC suite[a] and XSEED.[b] Intensities were corrected for Lorentz and polarization effects and an empirical absorption correction was applied using Blessing's method as incorporated into the program SADABS.[c] Non-hydrogen atoms were refined with aniostropic thermal parameters and hydrogen atoms were included in idealized positions. Structures for **3** and **4** were rendered with POV-Ray in XSEED using 50% probability ellipsoids; 35% probability ellipsoids were used for the structure of **5**.

In the structure of **3**, the C3 linker that connects the two [NHC]Cu fragments related by C2 symmetry was modeled at 50% occupancy due to this crystallographic symmetry element. Unique C28, C29, and C30 positions were identified and were treated by setting thermal parameters for C28 and C30 were set to be equal and related C-C distances within the symmetry-related C3 linker were constrained to be similar with the SADI commmand. Preliminary refinement of **4** showed the presence of a badly disordered fluorobenzene solvent molecule that was treated with the SQUEEZE subroutine of Platon[d] which revealed 367 solvent e^- / cell corresponding to 0.92 molecules of fluorobenzene / dinuclear **4**. Furthermore, disorder in the C_4 linker was modeled with a 73 / 27 ratio of occupancies for C55A – C58A / C55B – C58B. Two distinct S2A and S2B (connected to C58A and C58B, respectively) positions were identified and modeled in the same 73 / 27 ratio of occupancies. Despite a few attempts at its collection, the structure of **5** suffers from non-optimal diffraction data quality so exact bond distances and angles from this structure should be viewed with caution. Nonetheless, distances about the linear [NHC]-Cu-S core are very similar to those of **4**.

References for X-ray structure refinement details

(a) SHELXTL-PC, Vers. 5.10; 1998, Bruker-Analytical X-ray Services, Madison, WI; G. M. Sheldrick, SHELX-97, Universität Göttingen, Göttingen, Germany.

(b) L. Barbour, XSEED, 1999.

(c) SADABS; G. M. Sheldrick, 1996, based on the method described in R. H. Blessing, *Acta Crystallogr., Sect. A*, 1995, **51**, 33.

(d) Spek, A. L. *Acta Crystallogr.* **1990**, *A46*, C-34.

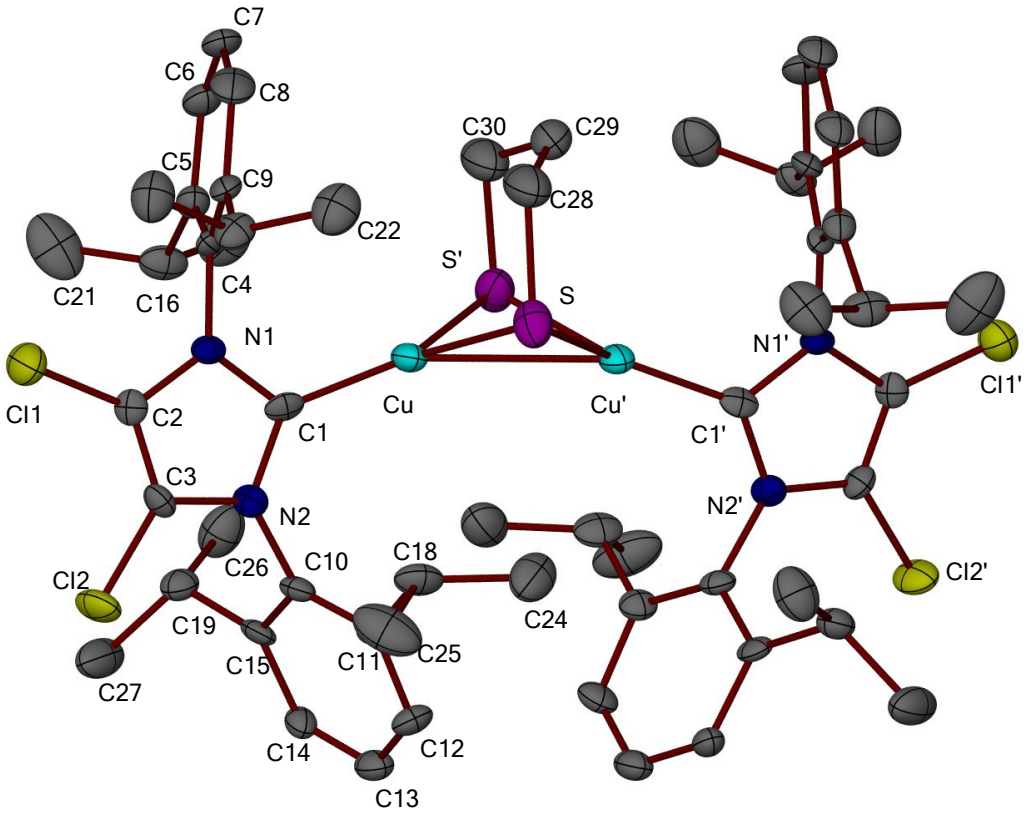

Figure S19. ORTEP diagram of $\{[Cl_2IPr]Cu\}_2(\mu\text{-}S(CH_2)_3S)$ (**3**) (all H atoms omitted; thermal ellipsoids represented at the 50% probability level). Selected bond distances (Å) and angles (deg): Cu-Cu' 2.8387(15), Cu-C1 1.887(6), Cu-S 2.2721(18), Cu-S' 2.362(2), C1-Cu-S 143.02(18), C1-Cu-S' 122.56(18), S-Cu-S' 93.76(7), Cu-S-Cu' 75.52(6).

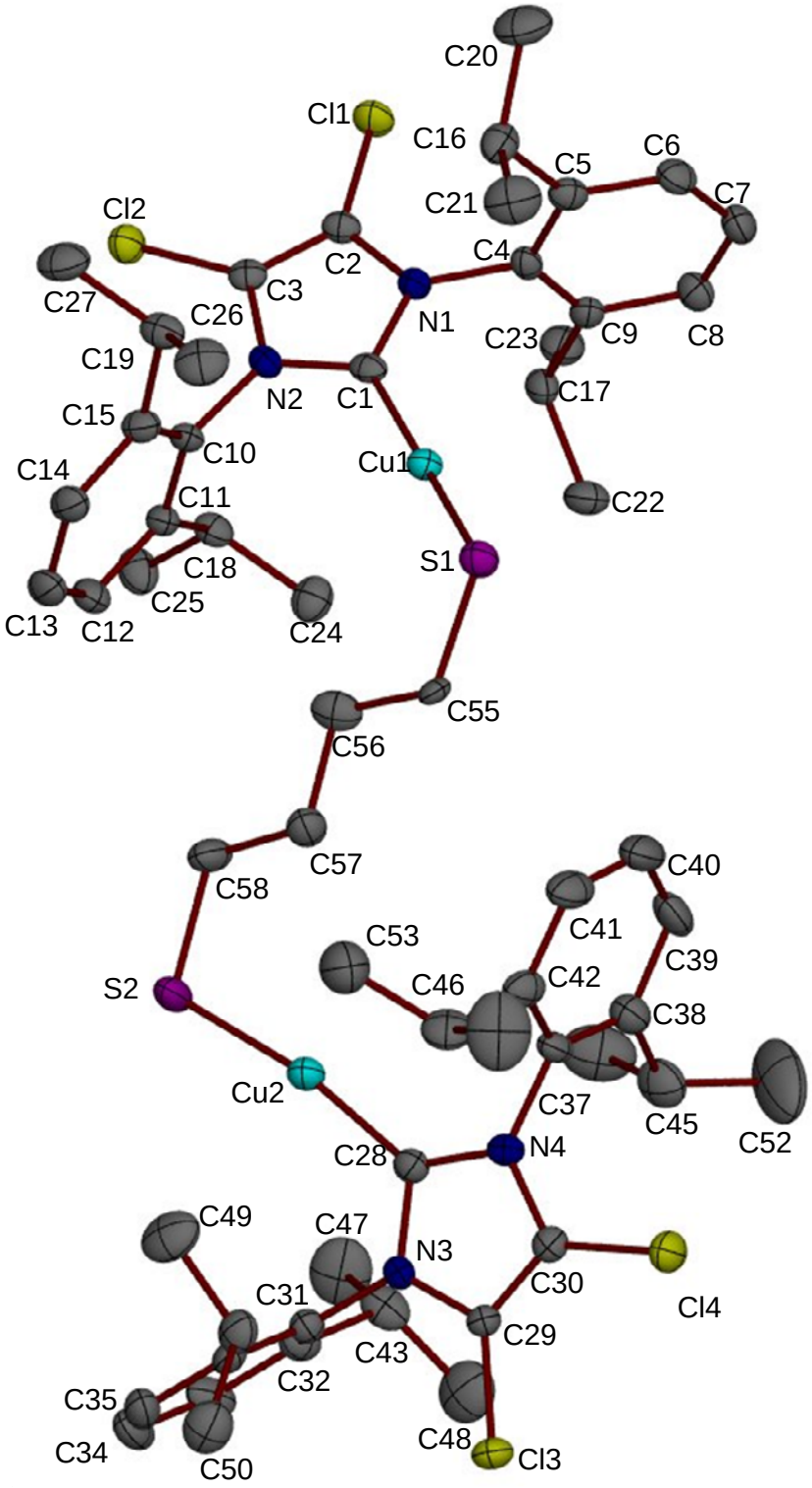

Figure S20. ORTEP diagram of {[Cl_2IPr]Cu}$_2$(μ-S$(CH_2)_4$S) (**4**) (all H atoms omitted; thermal ellipsoids represented at the 50% probability level). Selected bond distances (Å) and angles (deg): Cu1-C1 1.888(3), Cu1-S1 2.1293(10), Cu2-C28 1.894(3), Cu2-S2 2.148(3), C1-Cu1-S1 171.89(10), C28-Cu2-S2 170.06(12).

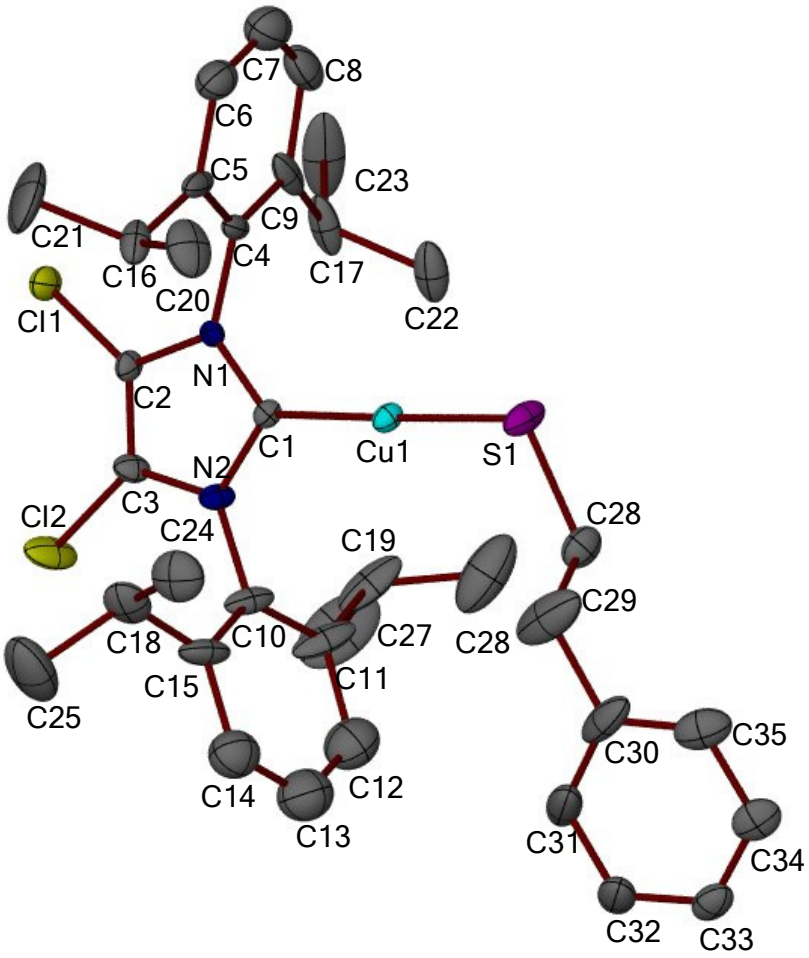

Figure S21. ORTEP diagram of [Cl_2IPr]Cu-SCH_2CH_2Ph) (**5**) (all H atoms omitted; thermal ellipsoids represented at the 35% probability level). Selected bond distances (Å) and angles (deg): Cu1-C1 1.891(5), Cu1-S1 2.130(2), S1-C28 1.858(6), C1-Cu1-S1 178.56(15), C28-S1-Cu1 106.7(2).